0026-895X/11/7903-472–478$20.00
MOLECULAR PHARMACOLOGY
Copyright © 2011 The American Society for Pharmacology and Experimental Therapeutics
Mol Pharmacol 79:472–478, 2011

Vol. 79, No. 3
69336/3663716
Printed in U.S.A.

The Novel UDP Glycosyltransferase 3A2: Cloning, Catalytic Properties, and Tissue Distribution

Peter I. MacKenzie, Anne Rogers, David J. Elliot, Nuy Chau, Julie-Ann Hulin, John O. Miners, and Robyn Meech

The Department of Clinical Pharmacology, Flinders University School of Medicine, Flinders Medical Centre, Bedford Park, Australia

Received October 12, 2010; accepted November 18, 2010

ABSTRACT

The human UDP glycosyltransferase (UGT) 3A family is one of three families involved in the metabolism of small lipophilic compounds. Members of these families catalyze the addition of sugar residues to chemicals, which enhances their excretion from the body. The UGT1 and UGT2 family members primarily use UDP glucuronic acid to glucuronidate numerous compounds, such as steroids, bile acids, and therapeutic drugs. We showed recently that UGT3A1, the first member of the UGT3 family to be characterized, is unusual in using UDP *N*-acetylglucosamine as sugar donor, rather than UDP glucuronic acid or other UDP sugar nucleotides (*J Biol Chem* **283:**36205–36210, 2008). Here, we report the cloning, expression, and characterization of UGT3A2, the second member of the UGT3 family. Like UGT3A1, UGT3A2 is inactive with UDP glucuronic acid as sugar donor. However, in contrast to UGT3A1, UGT3A2 uses both UDP glucose and UDP xylose but not UDP *N*-acetylglucosamine to glycosidate a broad range of substrates including 4-methylumbelliferone, 1-hydroxypyrene, bioflavones, and estrogens. It has low activity toward bile acids and androgens. UGT3A2 transcripts are found in the thymus, testis, and kidney but are barely detectable in the liver and gastrointestinal tract. The low expression of UGT3A2 in the latter, which are the main organs of drug metabolism, suggests that UGT3A2 has a more selective role in protecting the organs in which it is expressed against toxic insult rather than a more generalized role in drug metabolism. The broad substrate and novel UDP sugar specificity of UGT3A2 would be advantageous for such a function.

Introduction

Many lipophilic chemicals are metabolized to water-soluble products via β-linkage with hexose groups such as glucose, glucuronic acid, galactose, and xylose (Mackenzie et al., 2005). The UDP glycosyltransferases (UGT) that catalyze these reactions use UDP sugars as the donor, and functional groups including hydroxyl, carboxyl, amine, thiol, and carbon groups on the lipophilic chemical as acceptor. Conjugation with hexose groups generally reduces the biological activity of the aglycone and facilitates its removal from cells and from the body in urine and bile (Miners and Mackenzie, 1991; Meech and Mackenzie, 1997; Radominska-Pandya et al., 1999; Tukey and Strassburg, 2000; Miners et al., 2004). This function of UGTs is central to their pivotal roles in protecting cells against the accumulation of lipophilic toxins and unwanted products of metabolism and in modulating cell signaling pathways controlled by chemical ligands.

UDP glycosyltransferases are present in animals, plants, and microorganisms (http://www.flinders.edu.au/medicine/sites/clinical-pharmacology/ugt-homepage.cfm). In general, it seems that UDP glucuronic acid is the preferred sugar donor for conjugation of lipophilic chemicals in vertebrates, whereas UDP glucose is the preferred sugar donor in invertebrates, plants, and microorganisms. The human genome contains four UGT families. The UGT1 and UGT2 families contain 9 and 10 members, respectively. Characterization of the catalytic properties of all members of these two families (Mackenzie et al., 1997) shows that, although the substrate profile for each member is unique, some substrates are almost exclusively metabolized by one UGT, whereas other substrates are metabolized by several UGTs (Miners et al., 2010). This broad, overlapping substrate selectivity is well suited to a role in modulating the concentrations of chemicals in cells and hence in protecting organs and tissues against the toxic effects of chemical overload. The UGT1 and UGT2 families preferentially use UDP glucuronic acid as a sugar

This work was supported by the National Health and Medical Research Council (NHMRC) of Australia [NHMRC Senior Principal Research Fellowship (to P.I.M.).

Article, publication date, and citation information can be found at http://molpharm.aspetjournals.org.

doi:10.1124/mol.110.069336.

ABBREVIATIONS: UGT, UDP glycosyltransferase; HEK, human embryonic kidney; 4-MU, 4-methylumbelliferone; GAPDH, glyceraldehyde-3-phosphate dehydrogenase; PCR, polymerase chain reaction; HPLC, high-performance liquid chromatography; GAG, glycosaminoglycan.

donor to aid in the removal of a myriad of endogenous and xenobiotic compounds. In contrast, relatively little is known about the function of the UGT3 family, which consists of two members, UGT3A1 and UGT3A2. We have shown that UGT3A1 preferentially uses UDP *N*-acetylglucosamine in conjugation reactions with several substrates, including ursodeoxycholic acid and 17-estradiol (Mackenzie et al., 2008). However, the second member, UGT3A2 has not been characterized, although its similarity in sequence to UGT3A1 (78%) suggested that it was also a UDP *N*-acetylglucosaminyltransferase (Meech and Mackenzie, 2010). The fourth UGT family, UGT8, contains only one member that uses UDP galactose to galactosidate ceramide, a key step in the synthesis of brain sphingolipids (Bosio et al., 1996). This UGT seems not to be involved in xenobiotic metabolism, because other substrates have not been identified.

In mammals, UGTs are located in the membranes of the endoplasmic reticulum and nuclear envelope. Each cell, tissue, or organ expresses a specific subset of UGTs, which is appropriate for its role in regulating the concentrations of chemical toxins and/or ligands involved in cell signaling pathways. Commensurate with their dominant role in the metabolism and elimination of lipophilic compounds from the body, the liver, kidney, and gastrointestinal tract contain most members of the UGT1 and UGT2 families. However, there are differences in UGT content between these organs, as exemplified by the presence of UGT1A7, UGT1A8, and UGT1A10 in the gastrointestinal tract and their absence from the liver and kidney (Mojarrabi and Mackenzie, 1998). Other organs and tissues generally contain lower amounts of UGT and/or have a more restricted complement of UGTs. They may also contain UGTs that are expressed poorly in the liver or gastrointestinal tract, for example, UGT2A1 and UGT2A2, which are mainly found in nasal mucosa (Sneitz et al., 2009). The selective expression of UGTs in a tissue or organ, compared with the liver, kidney, and gastrointestinal tract, may reflect a special need for selective glucuronidating capacity in that tissue or organ. For example, UGT2A1 and 2A2 glucuronidate phenolic compounds (Sneitz et al., 2009), which may aid in odorant signal termination, and steroid-responsive breast, prostate, and adipose tissues express the steroid-metabolizing UGT2B15 or UGT2B17 (Barbier and Bélanger, 2008; Ohno and Nakajin, 2009), which have been shown to be involved in steroid-signal termination (Chouinard et al., 2008). Hence, characterization of both the catalytic properties and tissue distribution of all UGTs is important in elucidating their role in endogenous biochemistry and in drug metabolism and toxicity.

Based on an analysis of the human genome, UGT3A2 is the last member of the UGT superfamily whose function and tissue distribution have not been characterized. Here we report the cloning and expression of UGT3A2 and demonstrate that it is a xenobiotic-conjugating enzyme with a broad substrate selectivity but a unique UDP sugar selectivity and tissue distribution.

Materials and Methods

Materials. Radioactive and nonradioactive UDP sugars were obtained from the following sources: [^{14}C]UDP-galactose, -glucuronic acid, and -xylose were from PelkinElmer Life and Analytical Sciences (Waltham, MA); [^{14}C]UDP-glucose and -*N*-acetylglucosamine were from GE Healthcare (Chalfont St. Giles, Buckinghamshire, UK); UDP-glucose, -glucuronic acid, -galactose, and -*N*-acetylglucosamine were from Sigma-Aldrich (St. Louis, MO); and UDP-xylose was from Carbosource Services (Athens, GA). 4-MU-glucoside, -glucuronide, -galactoside, and -xyloside were purchased from Sigma-Aldrich. All other reagents and solvents were of analytical reagent grade.

cDNA Cloning and Expression. RNA from human embryonic kidney (HEK) 293 cells was used as template to synthesize first strand cDNA with the Superscript First Strand Synthesis System (Invitrogen, Carlsbad, CA). The UGT3A2 coding region (GenBank accession number NM_174914) was amplified from this cDNA using the forward primer 5′-AGCATGGCTGGGCAGCGAGTGCTT-3′ and the reverse primer 5′-TGGCCTTATGTCTCCTTCACCTTT-3′. The UGT3A2 initiation and stop codons in the forward and reverse primers, respectively, are underlined. PCR was performed in a volume of 50 μl with 200 ng of cDNA, and 0.5 μM concentration of the forward and reverse primers and the DNA polymerase Pfu Turbo (Stratagene, La Jolla, CA). The cycling parameters consisted of one cycle at 95°C for 2 min, 35 cycles of 95°C for 0.5 min, 60°C for 0.5 min, and 72°C for 2 min followed by a single 5-min cycle at 72°C. After electrophoresis on a 1% agarose gel, PCR products were excised and purified from the gel using the QIAquick gel extraction kit (QIAGEN, Valencia, CA) and subcloned into the pCR2.1 shuttle vector (Invitrogen) for sequencing. Sequencing revealed the presence of two species of UGT3A2 cDNA, a full-length sequence corresponding to NM_174914, and a sequence missing exon 2, corresponding to GenBank accession number NM_001168316. Both cDNAs were cloned into the pEF-IRESpuro6 expression vector, which contains a puromycin resistance gene (Hobbs et al., 1998). Expression vectors containing UGT3A2 in either the forward or reverse direction were transfected into HEK293T cells, and cell lines stably expressing UGT3A2 proteins were selected with puromycin (2 μg/ml). Expressed UGT3A2 was analyzed by Western blotting and enzyme activity assays.

Western Blotting. Proteins in lysates from HEK293T cells stably expressing UGT3A cDNA were separated on SDS-polyacrylamide gels and transferred to nitrocellulose membranes as described previously (Udomuksorn et al., 2007; Mackenzie et al., 2008). UGT3A2 protein was detected with UGT3A2 antibody and a secondary goat anti-rabbit antibody conjugated with peroxidase (Neomarkers; ThermoFisher Scientific, Fremont, CA). Immunocomplexes were visualized with the Supersignal West Pico chemiluminescent kit (ThermoFisher Scientific). The UGT3A2 antibody was prepared using amino acids 71 to 124 as antigen. This region was amplified from the UGT3A2 expression vector by PCR with 5′- GTAGGATCCGAAAAATCATATCAAGTTATC-3′ and 5′-GTACTCGAGTCTTCCTTCGATAAAATGACTGCACTGCAACGC-3′ as the forward and reverse primers, respectively. The BamH1 and Xho1 sites of the forward and reverse primers, respectively (underlined), were used to clone the PCR product into the pET23a bacterial expression vector, which introduces a six-histidine C-terminal tag to proteins (Novagen, Madison, WI). *Escherichia coli* (BL21-DE3) was transformed with this construct and UGT3A2 antigen was purified on a nickel-nitrilotriacetic acid column (QIAGEN). The purified antigen was used to prepare antibody in rabbits.

Quantitative PCR. The FirstChoice Human Total RNA Survey Panel (Ambion, Austin, TX) was used as template to quantify levels of UGT3A2 transcripts in various human tissues with the Rotor-Gene 300 (QIAGEN) thermal cycler. The forward and reverse primers specific for UGT3A2 were 5′-CATATCAAGTTATCAGTTGGCTTG-3 and 5′-ACTGCACTGCAACGCCAAGTA-3′, which correspond to nucleotides 218 to 241 and 346 to 366 of UGT3A2, respectively. The cycling parameters consisted of one cycle at 95°C for 15 min and then 40 cycles of 95°C for 10 s, 59°C for 15 s, and 72°C for 20 s. UGT3A2 plasmid was used as standard to determine transcript copy number.

Enzyme Assays. For assays to assess substrate preference, glycosidation reactions were performed as described previously (Mack-

enzie et al., 2008). In brief, incubations at 37°C for 1 h contained 100 mM phosphate buffer, pH 7.5, 4 mM magnesium chloride, 100 μg of HEK293T cell lysate, 200 μM aglycone, and 2 mM [^{14}C]UDP-sugar (0.1 μCi/mmol). Radioactive products were separated by thin-layer chromatography (Mackenzie et al., 2008) and quantified by exposure to a Phosphor Screen (GE Healthcare), which was scanned with a Typhoon 9400 scanner (GE Healthcare). Standard curves with known amounts of [^{14}C]UDP-sugar were constructed to quantify product formation. All reactions were carried out under conditions to give linear rates with respect to incubation time and protein concentration.

Kinetic studies with 4-MU and each of the UDP sugars used the same incubation conditions as those described for the activity screening experiments, except the incubation time was 15 min, and nonradiolabeled UDP sugars were used. Rates of 4-MU glycoside formation were determined at 9 or 10 4-MU concentrations over the ranges 10 to 250 μM (UDP-glucose as cofactor) or 30 to 1000 μM (UDP-galactose and UDP-xylose as cofactors). UDP-glucose and UDP-xylose kinetics were also characterized with 4-MU (2 mM) as the fixed substrate; incubations included nine UDP-sugar concentrations in the range of 25 to 5000 μM. All incubations were performed in duplicate (<10% variance between duplicate samples). 4-MU glycoside concentrations in incubation samples from kinetic experiments were analyzed by HPLC. Chromatography was performed with an Agilent 1100 HPLC system fitted with a NovaPak C18 column (3.9 × 150 mm, 4 μm particle size; Waters Corporation, Milford, MA) with UV detection at 316 nm. The mobile phase consisted of an aqueous component of 10 mM triethylamine (adjusted to pH 2.5 with perchloric acid), and 10% acetonitrile (A), and acetonitrile (B). Mobile phase was delivered at a flow rate of 1 ml/min. For 4-MU glucoside and 4-MU galactoside, initial conditions were 100% A/0% B held for 5.5 min, after which time the composition was changed to 65% A/35% B for 1 min before returning to the initial conditions. Retention times for 4-MU galactoside and 4-MU glucoside were 5.1 and 6.3 min, respectively. For 4-MU xyloside, initial conditions were 90% A/10% B held for 3 min, followed by 70% A/30% B for 1 min before returning to the initial conditions. The retention time for 4-MU xyloside was 2.5 min. The concentration of 4-MU conjugate was determined by comparison of peak areas with those of a calibration curve constructed under the same conditions using authentic individual 4-MU conjugates. Because the formation of each 4-MU glycoside exhibited hyperbolic kinetics, kinetic constants were derived by fitting the Michaelis-Menten equation to experimental data (EnzFitter; Biosoft, Ferguson, MO).

Results

Cloning and Expression of UGT3A2. The UGT3A family, consisting of two adjacent genes of seven exons on chromosome 5p13.2, was first identified in databases of the Human Genome Project in 2000 (●Authors et al., 2001●). Because initial studies using PCR screening of various cell lines with UGT3A2-specific primers revealed low levels of UGT3A2 mRNA in HEK293 cells (data not shown), this cell line was used to clone the UGT3A2 cDNA. Recombinant UGT3A2 protein, when overexpressed in HEK293 cells, has an apparent molecular mass of 53 kDa (Fig. 1, lane 3). Despite low but detectable levels of endogenous UGT3A2 transcripts in HEK293 cells, UGT3A2 protein was not detected in untransfected cells (Fig. 1, lane 1) or in cells ectopically expressing UGT3A1 (used as a control to demonstrate the specificity of the UGT3A2 antibody) (Fig. 1, lane 2). The recombinant UGT3A2del-exon2 protein, which is missing the 34 amino acids of exon 2, was also overexpressed by transfection of HEK293 cells. This shorter protein migrated with an apparent molecular mass of approximately 49 kDa (Fig. 1, lane 4).

Catalytic Properties of UGT3A2. The two members of the UGT3 family are 78% identical in sequence. Because UGT3A1 uses UDP-*N*-acetylglucosamine as sugar donor, we initially explored the hypothesis that UGT3A2 may also function as a UDP *N*-acetylglucosaminyltransferase. However, preliminary screens with a variety of potential substrates and UDP *N*-acetylglucosamine did not reveal an activity for UGT3A2 (data not shown). Both proteins contain a signal peptide, signature sequence, transmembrane domain and putative ER retention signal (Fig. 2). A more detailed comparison between the amino acid sequences of the two UGT3A proteins revealed that the putative substrate-binding domain (residues 23–250) and UDP sugar-binding domain (residues 251–486) of the two proteins vary by 22 and 20%, respectively. This contrasts to members of the UGT1A and UGT2 families, in which the putative substrate-binding domain is much less conserved than the putative UDP sugar-binding domain. In the UGT1A family, the putative UDP sugar-binding domain is identical between all nine members of this family, whereas their putative substrate-binding domains often vary by >50%. Likewise, members of the UGT2B family have much less variation in their UDP sugar-binding domains, as exemplified by a comparison between UGT2B4 and UGT2B7, in which their putative substrate-binding and UDP sugar-binding domains vary by 18 and 8%, respectively (data not shown). This unexpected large variation in the putative UDP sugar-binding domains of UGT3A1 and UGT3A2 compared with the UGT1A and UGT2 families prompted us to investigate whether UGT3A2 may have the capacity to use other UDP sugars in conjugation reactions. Indeed, preliminary screens with other UDP sugars revealed that UDP-glucose and UDP-xylose were effective sugar donors in UGT3A2-catalyzed glycosidations (see below).

UGT3A2 was active in the glucosylation of several hydroxylated xenobiotics including 4-MU, 1-hydroxypyrene, 7-hydroxycoumarin, and 1-naphthol, and the bioflavones, naringenin, genistein, and chrysin. It also glucosidated estrogens such as 17α-ethinylestradiol, 17β-estradiol, and diethylstilbestrol. However, UGT3A2 was inactive toward androgens and bile

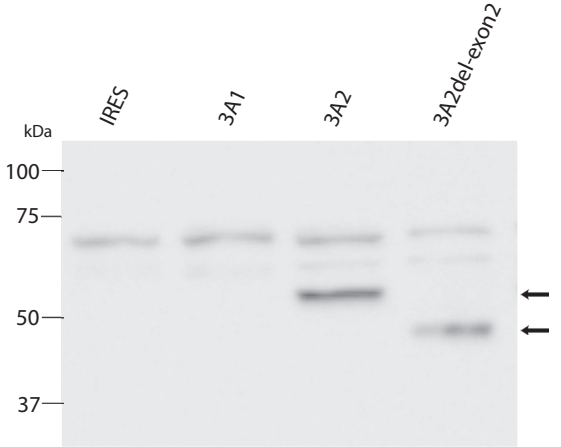

Fig. 1. Expression of UGT3A in HEK293T cells. Lysates of HEK293 cells transfected with UGT3A1, UGT3A2, and UGT3A2del-exon2 cDNAs were examined by Western blotting with an antibody specific for UGT3A2. The presence of UGT3A2 and UGT3A2del-exon2 protein is denoted by arrows. The molecular weight markers are indicated on the left.

acids with UDP-glucose as the cofactor (Table 1). UGT3A2 could also use UDP-xylose to conjugate the above substrates (Table 1) but was inactive when UDP glucuronic acid and UDP *N*-acetylglucosamine were used as sugar donors (Fig. 3). Although UGT3A2 was active with UDP-galactose as cofactor, its activity with this sugar donor was substantially less than with UDP-glucose and UDP-xylose. For example, the rates of 4-MU xylosidation and galactosidation were 60 and 2%, respectively, of that for glucosidation, when incubations were conducted with 2 mM UDP-sugar for 15 min at 37°C.

To further examine the enzymatic characteristics of UGT3A2, its relative glycosidation activity with the three separate cofactors (UDP-galactose, UDP-glucose, and UDP-xylose) was characterized kinetically with 4-MU as the aglycone using an HPLC method that measured formation of the individual galactoside, glucoside, and xyloside conjugates. Formation of 4-MU-galactoside, 4-MU-glucoside, and 4-MU-xyloside followed hyperbolic kinetics that were well described by the single-enzyme Michaelis-Menten equation (Fig. 4). Derived kinetic constants are given in Table 2. 4-MU-glucoside formation exhibited both the lowest apparent K_m and highest V_{max} values. As a consequence, the intrinsic clearance (CL_{int}, calculated as V_{max}/K_m) for 4-MU-glucoside was 2.4- and 80-fold higher than the intrinsic clearances of 4-MU-xyloside and 4-MU-galactoside, respectively. It should be noted, however, that 4-MU-glucoside was also detected as a product in incubations of 4-MU with UDP-galactose, presumably because of the presence of UDP-glucose as a contaminant in the commercial source of UDP-galactose. Thus, K_m and V_{max} values for 4-MU-galactoside may be over- and underestimated, respectively, as a consequence of competition by the contaminating cofactor.

UDP-glucose and UDP-xylose kinetics were additionally characterized with 4-MU as the fixed substrate. Both followed weak negative cooperative kinetics, which were modeled by the Hill equation. Derived values of S_{50}, V_{max}, and n (the Hill coefficient) were 357 ± 11 μM, 25,480 ± 242 pmol/min · mg, and 0.86 ± 0.01, respectively, for UDP-glucose, and 631 ± 21 μM, 3100 ± 42 pmol/min · mg, and 0.90 ± 0.01, respectively for UDP-xylose. UDP-galactose kinetics were not characterized because of the presumed contamination with the alternate sugar donor UDP-glucose. It should be noted that UDP-glucuronic acid also exhibits negative cooperative kinetics with UGT1A9 and UGT2B7 as the enzyme sources and 4-MU as the fixed substrate (Tsoutsikos et al., 2004).

In contrast to UGT3A2, cells transfected with UGT3A2del-exon2 cDNA synthesized a 49-kDa protein (Fig. 1, lane 4) that was devoid of glycosidation activity. The UGT3A2del-exon2 variant is missing all 34 amino acids of exon 2, including His35, the presumptive catalytic base required for catalysis (Kubota et al., 2007; Kerdpin et al., 2009).

Distribution of UGT3A2. Transcripts encoding UGT3A2 were detected in human thymus, testis, and kidney, as assessed by quantitative PCR using 20 normal human tissue samples, each of which contained a pool of RNA from 3 donors (Fig. 5). Only traces of transcript were detected in the liver, gastrointestinal tract, and other tissue samples.

Discussion

Although the substrate profile, catalytic properties, and tissue distribution of most human UGTs have been extensively characterized, this is the first report describing the function and distribution of UGT3A2. In common with UGT1 and UGT2 enzymes, UGT3A2 has a molecular mass in the 50- to 60-kDa range and broad substrate specificity, with the capacity to glycosidate a range of xenobiotics, including 4-MU, the classic "universal" substrate of most UGT1 and UGT2 forms (Uchaipichat et al., 2004). The kinetic parame-

```
3A2      1 MAGQRVLLLVGFLLPGVLLSEAAKILTISTVGGSHYLLMDRVSQILQDHGHNVTMLNHKR
3A1      1 MVGQRVLLLVAFLLSGVLLSEAAKILTISTLGGSHYLLLDRVSQILQEHGHNVTMLHQSG
           * ******** *** *************** ******* ******** ********

3A2     61 GPFMPDFKKEEKSYQVISWLAPEDHQREFKKSFDFFLEETLGGRGKFENLLNVLEYLALQ
3A1     61 KFLIPDIKEEEKSYQVIRWFSPEDHQKRIKKHFDSYIETALDGRKESEALVKLMEIFGTQ
               ** * ******** *  *****   ** **   *  * **   * *    *    *

3A2    121 CSHFLNRKDIMDSLKNENFDMVIVETFDYCPFLIAEKLGKPFVAILSTSFGSLEFGLPIP
3A1    121 CSYLLSRKDIMDSLKNENYDLVFVEAFDFCSFLIAEKLVKPFVAILPTTFGSLDFGLPSP
           **  * ************ * * ** ** * ******* ******* * **** **** *

3A2    181 LSYVPVFRSLLTDHMDFWGRVKNFLMFFSFCRRQQHMQSTFDNTIKEHFTEGSRPVLSHL
3A1    181 LSYVPVFPSLLTDHMDFWGRVKNFLMFFSFSRSQWDMQSTFDNTIKEHFPEGSRPVLSHL
           ******* ********************** * *  ************* **********

3A2    241 LLKAELWFINSDFAFDFARPLLPNTVYVGGLMEKPIKPVPQDLENFIAKFEDSGFVLVTL
3A1    241 LLKAELWFVNSDFAFDFARPLLPNTVYIGGLMEKPIKPVPQDLDNFIANFGDAGFVLVAF
           ******** ****************** *************** **** * * *****

3A2    301 GSMVNTCQNPEIFKEMNNAFAHLPQGVIWKCQCSHWPKDVHLAANVKIVDWLPQSDLLAH
3A1    301 GSMLNTHQSQEVLKKMHNAFAHLPQGVIWTCQSSHWPRDVHLATNVKIVDWLPQSDLLAH
           *** ** *  *  * * ************ ** **** ***** ****************

3A2    361 PSIRLFVTHGGQNSIMEAIQHGVPMVGIPLFGDQPENMVRVEAKKFGVSIQLKKLKAETL
3A1    361 PSIRLFVTHGGQNSVMEAIRHGVPMVGLPVNGDQHGNMVRVVAKNYGVSIRLNQVTADTL
           ************** **** ******* *  ***  ***** **  **** *    * **

3A2    421 ALKMKQIMEDKRYKSAAVAASVILRSHPLSPTQRLVGWIDHVLQTGGATHLKPYVFQQPW
3A1    421 TLTMKQVIEDKRYKSAVVAASVILHSQPLSPAQRLVGWIDHILQTGGATHLKPYAFQQPW
            * ***  ******** ******* * **** ********* ************ *****

3A2    481 HEQYLLDVFVFLLGLTLGTLWLCGKLLGMAVWWLRGARKVKET
3A1    481 HEQYLIDVFVFLLGLTLGTMWLCGKLLGVVARWLRGARKVKKT
           ***** ************* ********    ********* *
```

Fig. 2. Comparison of UGT3A1 and UGT3A2 protein sequences. UGT3A2 is aligned above UGT3A1, and identical residues are indicated by an asterisk. The signal peptide and putative transmembrane regions are highlighted in gray. The lysine residues of the C-terminal dilysine motif are in boldface type and underlined. The signature sequence, which defines the UGT superfamily, is highlighted in boldface type.

ters for UGT3A2 catalyzed 4-MU-glucoside formation (K_m = 82 μM and V_{max} = 3.9 nmol/min · mg) are comparable with those of UGT1 and UGT2 enzymes for 4-MU glucuronidation, measured under similar assay conditions (e.g., K_m or S_{50} values of 59, 78, 13, and 462 μM and V_{max} values of 0.4, 82, 8.3, and 1.0 nmol/min · mg for UGT1A1, UGT1A6, UGT1A9, and UGT2B7, respectively) (Uchaipichat et al., 2004).

TABLE 1
Substrates of UGT3A2 expressed in HEK293T cells
UGT3A2 activities were assayed as described under *Materials and Methods*.

	Activity	
	UDP Glucose	UDP Xylose
	pmol · min^{-1} · mg lysate protein^{-1}	
Xenobiotic		
Drug		
Mycophenolic acid	453	607
Paracetamol	–	N.D.
Phenobarbital	–	N.D.
Sulfamethoxazole	–	N.D.
Ibuprofen	–	N.D.
Ketoprofen	–	N.D.
Tetracycline	–	N.D.
Chloramphenicol	–	N.D.
Bioflavones		
Naringenin	842	470
Genistein	659	523
Chrysin	403	352
Isorhamnetin	358	N.D.
Biochanin A	278	246
Acacetin	257	N.D.
Diadzein	235	N.D.
Formononetin	100	N.D.
4′-Hydroxyflavanone	39	N.D.
2′-Hydroxyflavanone	33	N.D.
Primuletin	28	N.D.
Baicalein	–	N.D.
Epigallocatechin gallate	–	N.D.
Morin	–	N.D.
4′-Hydroxyflavone	+	N.D.
2′-Hydroxyflavone	+	N.D.
3-Hydroxyflavone	–	N.D.
Kaempferol	+	N.D.
Quercetin	–	N.D.
Luteolin	+	N.D.
Epichatechin	–	N.D.
Other		
4-Methylumbelliferone	959	686
1-Hydroxypyrene	865	462
7-Hydroxycoumarin	760	311
8′-Hydroxyquinoline	594	222
1-Naphthol	570	205
4-Nitrophenol	225	82
Phenolthalein	21	N.D.
(−)Borneol	–	N.D.
Steroids		
17α-Ethinylestradiol	104	N.D.
17β-Estradiol	86	N.D.
Diethylstilbestrol	66	N.D.
Estrone	44	N.D.
Estriol	39	N.D.
17α-Estradiol	32	N.D.
Androsterone	–	N.D.
Testosterone	–	N.D.
Dihydrotestosterone	–	N.D.
Etiocholanolone	–	N.D.
Bile Acids		
Ursodeoxycholic acid	–	N.D.
Chenodeoxycholic acid	–	N.D.
Lithocholic acid	–	N.D.
Hyodeoxycholic acid	–	N.D.
α-Muricholic acid	–	N.D.
β-Muricholic acid	–	N.D.

+, low activity detected but not quantifiable by the thin-layer chromatography method; –, no activity; N.D., not determined.

UGT3A2 is also active toward estrogens but has little activity toward androgens and bile acids. However, unlike the other human UGTs, UGT3A2 preferentially uses UDP-glucose and UDP-xylose as sugar donors in glycosidation reactions. The preference for these UDP sugars is unique to this enzyme, because the major sugar donors for the other human UGTs are UDP glucuronic acid (UGT1 and UGT2 forms), UDP *N*-acetylglucosamine (UGT3A1), and UDP galactose (UGT8). The apparent affinities of UGT3A2, assessed as S_{50} values, for UDP-glucose (S_{50} of 357 μM) and UDP-xylose (S_{50} of 631 μM) are in the same range as those of UGT1 and UGT2 forms toward UDP glucuronic acid (e.g., S_{50} of 88 μM for UGT1A9 and K_m of 493 μM for UGT2B7) (Tsoutsikos et al., 2004).

Given that quite divergent UGTs (e.g., UGT1A and UGT2B forms, which may differ in sequence by >50%) have the same UDP-sugar preference, the finding that two closely related members of the same UGT family have different UDP-sugar specificities was unexpected. The functional significance of this is obscure, but in the case of UGT3A2, it may relate to the possibility of preserving UDP glucuronic acid for glycosaminoglycan (GAG) synthesis. GAGs are synthesized in most body tissues and have important roles in controlling cell growth and differentiation during embryogenesis and in the adult (Prydz and Dalen, 2000). Because the synthesis of these compounds is regulated by UDP glucuronic acid availability (Spicer et al., 1998; Lind et al., 1999), there is the potential for competition between drug glucuronidation and

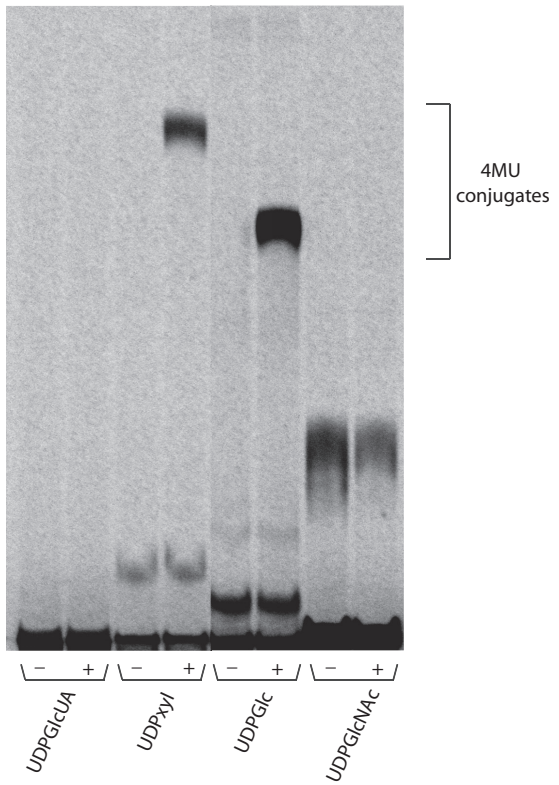

Fig. 3. UDP-sugar selectivity of UGT3A2. Various UDP sugars were used as cosubstrates in the glycosidation of 4-MU by lysates of HEK293T cells transfected with UGT3A2 cDNA in the forward (+) and reverse (−) orientations. An autoradiograph of the thin-layer chromatography plate containing 4-MU conjugates and unreacted UDP sugar and/or its breakdown products from assays with 250 μM substrate and 0.5 mM [^{14}C]UDP sugars is shown. Equal amounts of radiolabeled UDP sugar (0.4 μCi/mmol) were used in each reaction.

GAG synthesis for the intracellular pool of UDP glucuronic acid. Indeed, this principle underlies the use of 4-MU as a potent inhibitor of GAG synthesis (Kakizaki et al., 2004; Rilla et al., 2005), because 4-MU glucuronidation diverts UDP glucuronic acid from GAG biosynthetic pathways. This competition may be especially intense in tissues that have low levels of UDP glucose dehydrogenase, the enzyme that synthesizes UDP glucuronic acid from UDP glucose. In this situation, UDP glucose may be abundant, but UDP glucuronic acid may be limiting. It is interesting to note that the main UGT3A2-expressing organs, thymus, testis, and kidney, have levels of UDP glucose dehydrogenase that are significantly lower (approximately 5-fold) than that of the liver and gastrointestinal tract (Spicer et al., 1998). Hence, the use of UDP glucose, rather than UDP glucuronic acid, to inactivate and eliminate lipophilic chemicals in the thymus, testis, and kidney, would help to preserve GAG synthesis and alleviate any competition for the UDP glucuronic acid pool. Moreover, as the concentration of UDP glucose is usually greater than UDP glucuronic acid in those cells in which it

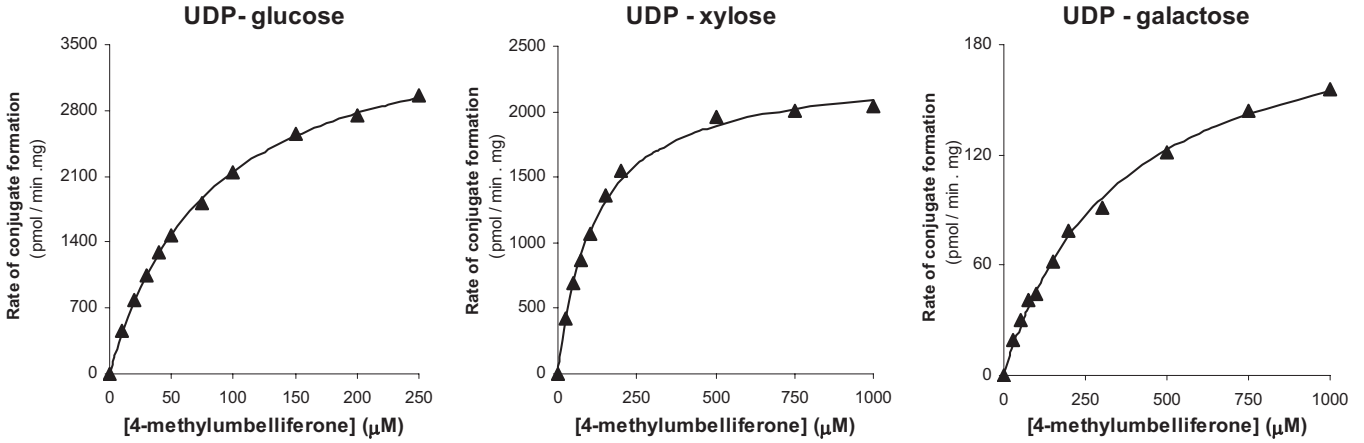

Fig. 4. Kinetic plots for 4-MU glycosidation by UGT3A2. Rates of conjugate formation verses substrate concentration plots with UDP-glucose, UDP-xylose, and UDP-galactose as cofactor are shown. Points (mean of duplicate estimates) are experimentally derived values, whereas curves are from model fitting.

TABLE 2

Derived kinetic parameters for 4-MU-galactoside, 4-MU-glucoside, and 4-MU-xyloside formation

Data presented as parameter ± S.E. of the parameter fit.

UDP-Sugar	Product	K_m	V_{max}	CL_{int}
		μM	$pmol \cdot min^{-1} \cdot mg^{-1}$	$\mu l \cdot min^{-1} \cdot mg^{-1}$
UDP-Galactose	4-MU-gal	348 ± 21	208 ± 5	0.6
UDP-Glucose	4-MU-glu	82 ± 1	3918 ± 26	48
UDP-Xylose	4-MU-xyl	116 ± 5	2332 ± 34	20

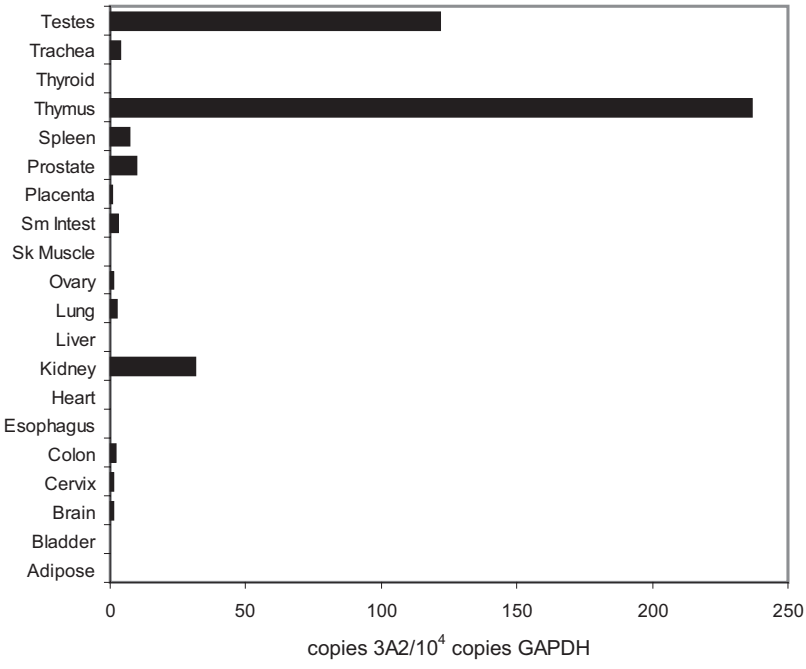

Fig. 5. Tissue distribution of UGT3A2. Levels of UGT3A2 RNA in different tissues as represented by a human tissue RNA panel were quantified as described under *Materials and Methods*. The copies of UGT3A2 mRNA per copy of GAPDH transcript in each tissue are shown.

has been measured (Gainey and Phelps, 1972), it is likely that glucosylation may be less subject to fluctuating levels of UDP sugars than glucuronidation in extrahepatic tissues. Indeed, evidence that the supply of UDP glucuronic acid is rate-limiting for androgen glucuronidation in the prostate has been provided (Wei et al., 2009).

In contrast to most members of the UGT1 and UGT2 families, UGT3A2 mRNA is not found in two of the major organs of drug metabolism, the liver and gastrointestinal tract, but is found in the kidney, thymus, and testis, as mentioned previously. Many members of the UGT1 and UGT2 families are expressed in the kidney at much higher levels than UGT3A2. These include UGT1A6, UGT1A9, and UGT2B7, whose mRNA levels are approximately 20-, 150-, and 120-fold greater than those of UGT3A2, respectively, based on data for these UGTs relative to levels of glyceraldehyde-3-phosphate dehydrogenase (GAPDH) (Ohno and Nakajin, 2009). Hence, it is unlikely that UGT3A2 contributes significantly to glycosidation of lipophilic chemicals in this organ. However, UGT3A2 is expressed at higher amounts than other UGTs in thymus and testis. Only UGT1A5, UGT2B4, and UGT2B7 have been detected in thymus (Ohno and Nakajin, 2009), but these are at levels approximately 31-, 9-, and 7-fold less then that of UGT3A2. Testis contains equivalent amounts of UGT3A2 and UGT2B15 but 18- and 35-fold less UGT2B4 and UGT2B17, respectively. The exact role of UGT3A2 in the thymus and testis is unknown but is most likely protective in nature, although a specific role in modulating ligand concentrations in signaling pathways cannot be excluded.

Finally, the discovery that UGT3A1 and UGT3A2 have divergent UDP sugar preferences provides a unique opportunity to identify the amino acids involved in UDP sugar selection via site-directed mutagenesis and analyses of chimeras of these two closely related UGTs. This approach is currently being pursued in our laboratory.

In summary, we demonstrate that UGT3A2 is a novel UDP glycosyltransferase with a unique UDP sugar selectivity, in that it has the capacity to covalently attach glucose and xylose to many foreign chemicals and estrogen-like compounds. Its high expression in the thymus and testis and its poor expression in the liver and gastrointestinal tract suggest a unique role for this enzyme in drug metabolism. Further substrate characterization and a more detailed examination of the expression of UGT3A2 in cells within the thymus and testis may help clarify this role.

Authorship Contributions

Participated in research design: Mackenzie, Miners, and Meech.

Conducted experiments: Mackenzie, Rogers, Elliot, Chau, Hulin, and Meech.

Performed data analysis: Mackenzie, Rogers, Elliot, Chau, Hulin, Miners, and Meech.

Wrote or contributed to the writing of the manuscript: Mackenzie, Elliot, Miners, and Meech.

References

Barbier O and Bélanger A (2008) Inactivation of androgens by UDP-glucuronosyltransferases in the human prostate. *Best Pract Res Clin Endocrinol Metab* **22:**259–270.

Bosio A, Binczek E, Le Beau MM, Fernald AA, and Stoffel W (1996) The human gene CGT encoding the UDP-galactose ceramide galactosyl transferase (cerebroside synthase): cloning, characterization, and assignment to human chromosome 4, band q26. *Genomics* **34:**69–75.

Chouinard S, Yueh MF, Tukey RH, Giton F, Fiet J, Pelletier G, Barbier O, and Bélanger A (2008) Inactivation by UDP-glucuronosyltransferase enzymes: the end of androgen signaling. *J Steroid Biochem Mol Biol* **109:**247–253.

Gainey PA and Phelps CF (1972) Uridine diphosphate glucuronic acid production and utilization in various tissues actively synthesizing glycosaminoglycans. *Biochem J* **128:**215–227.

Hobbs S, Jitrapakdee S, and Wallace JC (1998) Development of a bicistronic vector driven by the human polypeptide chain elongation factor 1alpha promoter for creation of stable mammalian cell lines that express very high levels of recombinant proteins. *Biochem Biophys Res Commun* **252:**368–372.

Kakizaki I, Kojima K, Takagaki K, Endo M, Kannagi R, Ito M, Maruo Y, Sato H, Yasuda T, Mita S, et al. (2004) A novel mechanism for the inhibition of hyaluronan biosynthesis by 4-methylumbelliferone. *J Biol Chem* **279:**33281–33289.

Kerdpin O, Mackenzie PI, Bowalgaha K, Finel M, and Miners JO (2009) Influence of N-terminal domain histidine and proline residues on the substrate selectivities of human UDP-glucuronosyltransferase 1A1, 1A6, 1A9, 2B7, and 2B10. *Drug Metab Dispos* **37:**1948–1955.

Kubota T, Lewis BC, Elliot DJ, Mackenzie PI, and Miners JO (2007) Critical roles of residues 36 and 40 in the phenol and tertiary amine aglycone substrate selectivities of UDP-glucuronosyltransferases 1A3 and 1A4. *Mol Pharmacol* **72:**1054–1062.

Lind T, Falk E, Hjertson E, Kusche-Gullberg M, and Lidholt K (1999) cDNA cloning and expression of UDP-glucose dehydrogenase from bovine kidney. *Glycobiology* **9:**595–600.

Mackenzie PI (2000) UDP Glucuronosyltransferase: Nomenclature and the Human Genome Project, 10th International Workshop on Glucuronidation and the UDP Glucuronosyltransferases; 22–25 April 2001; Hyogo, Japan.

Mackenzie PI, Bock KW, Burchell B, Guillemette C, Ikushiro S, Iyanagi T, Miners JO, Owens IS, and Nebert DW (2005) Nomenclature update for the mammalian UDP glycosyltransferase (UGT) gene superfamily. *Pharmacogenet Genomics* **15:**677–685.

Mackenzie PI, Owens IS, Burchell B, Bock KW, Bairoch A, Bélanger A, Fournel-Gigleux S, Green M, Hum DW, Iyanagi T, et al. (1997) The UDP glycosyltransferase gene superfamily: recommended nomenclature update based on evolutionary divergence. *Pharmacogenetics* **7:**255–269.

Mackenzie PI, Rogers A, Treloar J, Jorgensen BR, Miners JO, and Meech R (2008) Identification of UDP glycosyltransferase 3A1 as a UDP N-acetylglucosaminyltransferase. *J Biol Chem* **283:**36205–36210.

Meech R and Mackenzie PI (1997) Structure and function of uridine diphosphate glucuronosyltransferases. *Clin Exp Pharmacol Physiol* **24:**907–915.

Meech R and Mackenzie PI (2010) UGT3A: novel UDP-glycosyltransferases of the UGT superfamily. *Drug Metab Rev* **42:**43–52.

Miners JO and Mackenzie PI (1991) Drug glucuronidation in humans. *Pharmacol Ther* **51:**347–369.

Miners JO, Mackenzie PI, and Knights KM (2010) The prediction of drug-glucuronidation parameters in humans: UDP-glucuronosyltransferase enzyme-selective substrate and inhibitor probes for reaction phenotyping and in vitro-in vivo extrapolation of drug clearance and drug-drug interaction potential. *Drug Metab Rev* **42:**189–201.

Miners JO, Smith PA, Sorich MJ, McKinnon RA, and Mackenzie PI (2004) Predicting human drug glucuronidation parameters: application of in vitro and in silico modeling approaches. *Annu Rev Pharmacol Toxicol* **44:**1–25.

Mojarrabi B and Mackenzie PI (1998) Characterization of two UDP glucuronosyltransferases that are predominantly expressed in human colon. *Biochem Biophys Res Commun* **247:**704–709.

Ohno S and Nakajin S (2009) Determination of mRNA expression of human UDP-glucuronosyltransferases and application for localization in various human tissues by real-time reverse transcriptase-polymerase chain reaction. *Drug Metab Dispos* **37:**32–40.

Prydz K and Dalen KT (2000) Synthesis and sorting of proteoglycans. *J Cell Sci* **113:**193–205.

Radominska-Pandya A, Czernik PJ, Little JM, Battaglia E, and Mackenzie PI (1999) Structural and functional studies of UDP-glucuronosyltransferases. *Drug Metab Rev* **31:**817–899.

Rilla K, Siiskonen H, Spicer AP, Hyttinen JM, Tammi MI, and Tammi RH (2005) Plasma membrane residence of hyaluronan synthase is coupled to its enzymatic activity. *J Biol Chem* **280:**31890–31897.

Sneitz N, Court MH, Zhang X, Laajanen K, Yee KK, Dalton P, Ding X, and Finel M (2009) Human UDP-glucuronosyltransferase UGT2A2: cDNA construction, expression, and functional characterization in comparison with UGT2A1 and UGT2A3. *Pharmacogenet Genomics* **19:**923–934.

Spicer AP, Kaback LA, Smith TJ, and Seldin MF (1998) Molecular cloning and characterization of the human and mouse UDP-glucose dehydrogenase genes. *J Biol Chem* **273:**25117–25124.

Tsoutsikos P, Miners JO, Stapleton A, Thomas A, Sallustio BC, and Knights KM (2004) Evidence that unsaturated fatty acids are potent inhibitors of renal UDP-glucuronosyltransferases (UGT): kinetic studies using human kidney cortical microsomes and recombinant UGT1A9 and UGT2B7. *Biochem Pharmacol* **67:**191–199.

Tukey RH and Strassburg CP (2000) Human UDP-glucuronosyltransferases: metabolism, expression, and disease. *Annu Rev Pharmacol Toxicol* **40:**581–616.

Uchaipichat V, Mackenzie PI, Guo XH, Gardner-Stephen D, Galetin A, Houston JB, and Miners JO (2004) Human udp-glucuronosyltransferases: isoform selectivity and kinetics of 4-methylumbelliferone and 1-naphthol glucuronidation, effects of organic solvents, and inhibition by diclofenac and probenecid. *Drug Metab Dispos* **32:**413–423.

Udomuksorn W, Elliot DJ, Lewis BC, Mackenzie PI, Yoovathaworn K, and Miners JO (2007) Influence of mutations associated with Gilbert and Crigler-Najjar type II syndromes on the glucuronidation kinetics of bilirubin and other UDP-glucuronosyltransferase 1A substrates. *Pharmacogenet Genomics* **17:**1017–1029.

Wei Q, Galbenus R, Raza A, Cerny RL, and Simpson MA (2009) Androgen-stimulated UDP-glucose dehydrogenase expression limits prostate androgen availability without impacting hyaluronan levels. *Cancer Res* **69:**2332–2339.

Address correspondence to: Dr. Peter I. Mackenzie, Department of Clinical Pharmacology, Flinders Medical Centre, Bedford Park, SA 5042, Australia. E-mail: peter.mackenzie@flinders.edu.au